Selective determination of non-organophosphorus insecticide using DNA aptamer-based single-use biosensors

Mustafa Barış Koçer[1*]
Gözde Aydoğdu Tığ[2]
Şule Pekyardımcı[2]

[1] Department of Chemistry, Faculty of Science, Selçuk University, Konya, Turkey

[2] Department of Chemistry, Faculty of Science, Ankara University, Ankara, Turkey

Abstract

In the present study, we developed a disposable aptamer-based biosensor for rapid, sensitive, and reliable detection of acetamiprid (ACE). To improve the sensitivity of the aptasensor, poly-5-amino-2-mercapto-1,3,4-thiadiazole [P(AMT)] and gold nanoparticles (AuNPs) were progressively electrodeposited on the screen-printed electrode (SPE) surface by using cyclic voltammetry (CV) technique. For the determination of ACE, thiol-modified primary aptamer (Apt1) was selected by using the SELEX method and immobilized on the surface of the P(AMT) and AuNPs-modified SPE (SPE/P(AMT)/AuNPs) via Au–S bonding. Then, the surface-bound aptamer was incubated with ACE for 45 Min. After that, the biotin-labeled aptamer 2 (Apt2) was interacted with the ACE, then the enzyme-labeled step was performed. In this step, alkaline phosphatase (ALP) was bound to the surface through the interaction between Apt2 labeled with biotin and streptavidin (strep)–ALP conjugate. The determination of ACE was achieved by measuring the oxidation signal of α-naphthol, which is formed on the electrode surface through the interaction of ALP with α-naphthyl phosphate. The working range of the developed aptasensor was determined as 5×10^{-12}–5×10^{-10} mol L^{-1} with a low limit of detection (1.5 pmol L^{-1}). It was also found that the proposed aptasensor possessed great advantages such as low cost, good selectivity, and good reproducibility.

Keywords: *acetamiprid, aptamer, biosensor, electrochemistry, screen-printed electrode*

Abbreviations: *ACE, acetamiprid; AMT, 5-amino-2-mercapto-1,3,4-thiadiazole; Apt1, aptamer 1; Apt2, aptamer 2; AuNPs, gold nanoparticles; BSA, bovine serum albumin; CNTs, carbon nanotubes; CV, cyclic voltammetry; DEA, diethanolamine; DPV, differential pulse voltammetry; EIS, electrochemical impedance spectroscopy; ELISA, enzyme-linked immunosorbent assays; GC-MS, gas chromatography-mass spectrometry; HPLC, high-performance liquid chromatography; LOD, limit of detection; LOQ, limit of quantification; MWCNTs, multi walled carbon nanotubes; P(AMT), poly-5-amino-2-mercapto-1,3,4-thiadiazole; PBS, phosphate buffer solution; Ret, electron transfer resistance; RSD, relative standard deviation; ssDNA, single-stranded DNA; SEM, scanning electron microscopy; SPE, screen printed electrode; Strep-ALP, streptavidin-alkaline phosphatase; XPS, X-ray photoelectron spectroscopy.*

*Address for correspondence: *Mustafa Barış Koçer, MSc, Department of Chemistry, Faculty of Science, Selçuk University, Konya 42075, Turkey. Tel.: 903322233901; Fax: 903322412499; e-mail: mbariskocer@gmail.com.*

Additional supporting information may be found online in the Supporting Information section at the end of the article.

Received 20 March 2020; accepted 17 September 2020

DOI: 10.1002/bab.2039

Published online in Wiley Online Library (wileyonlinelibrary.com)

1. Introduction

Neonicotinoid insecticides, an alternative to organophosphates and carbamates, are commonly used in many parts of the world [1]. Neonicotinoids bind to nicotinic acetylcholine receptors (nAChRs) and function as nAChR agonists in the central nervous system of the insects [2]. Imidacloprid, dinotefuran, nitenpyram, thiacloprid, clothianidin, and acetamiprid (ACE) are the most commonly used neonicotinoid insecticides [3]. Among them, ACE, N-[(6-chloro-3-pyridyl)methyl]-N′-cyano-N-methyl-acetamidine, a broad-spectrum pesticide, is used as an alternative to other pesticides for the protection of crops from insects such as Coleoptera, Hemiptera, and Thysanoptera due to its relatively low toxicity to mammals [4]. It has been proved that it has good efficacy in combatting pests damaging crops; on the other hand, there are serious concerns about its extensive use is causing pollution of soil and water bodies as well as foods. Also, its frequent and extensive use poses health risks for people exposed to primary food and water contaminated by ACE. Thus, the development of new techniques with high selectivity and sensitivity for the detection of ACE in water

and food samples is of great importance for environmental protection and human health.

In the recent literature, analytical tools based on high-performance liquid chromatography (HPLC) [5], gas chromatography–mass spectrometry (GC–MS) [6], liquid chromatography–mass spectrometry [7, 8], and enzyme-linked immunosorbent assays (ELISA) [9] were developed for the analysis of ACE. Though these instrumental tools have significant advantages of high sensitivity and accuracy, they require specialized personnel and expensive instruments. Moreover, these analytical techniques are limited to laboratories and time consuming [10]. Therefore, it has become important to develop a fast, simple, highly selective, and sensitive method for monitoring and detection of ACE residues in wastewater samples and authentic samples [11].

In recent years, biosensor development for the analysis of pesticides such as ACE has attracted much attention [12]. Recently, synthetic receptors such as aptamers have been successfully used in biosensor technology to increase the specificity and chemical stability of the biosensors [13]. Aptamers are single-stranded DNA or RNA oligonucleotides that fold into a different three-dimensional conformation that can bind strongly and selectively to all kind of targets such as small molecules, macromolecules, and metal ions with high affinity [14, 15]. Aptamers are obtained using an *in vitro* selection technique named SELEX [16]. Aptamers have become one of the most important molecular recognition tools due to their unique properties such as easy to be modified, high water solubility, and easily synthesizable [17]. Aptamers can bind not only to proteins [18] but also to other molecules such as metal ions [19], and small molecules [20]. Compared with antibody, aptamers possess many merits such as easier storage and functionalization, simpler artificial synthesis and modification, lower cost, and better stability. [11]. Due to their distinctive properties, aptamers have attracted great attention for many applications [15, 21-24].

Biosensors using RNA or DNA aptamers as recognition elements are called aptasensors [25]. Aptasensors are being studied as a facile and versatile tool for the detection of different molecules such as heavy metals [26, 27], drugs [28, 29], and pesticides [30–32]. Electrochemical aptasensors are biosensors developed by immobilizing an aptamer on an electrically conductive substrate [33]. In recent years, the electrochemical aptasensors have attracted great attention due to their different features such as easier artificial synthesis, simplicity, high sensitivity and selectivity, more flexibility, ease storage, and low cost for target detection [25, 32, 34]. They also play a key role in the monitoring of quality and safety in food production with simple designs, fast response times, low costs, and high sensitivity, and in diagnosing diseases in clinical practice [35–37].

Nanomaterials represent a new class of materials that expand and improve the performance and applications of biosensing systems [38]. In recent years, nanomaterials have gained a great deal of interest in analytical chemistry and biochemistry due to their important properties such as good biocompatibility, strong adsorbability, high controllable size, and high catalytic activity [39]. Because of these advantages, they are frequently used in many fields such as pharmaceutical analysis, food safety, clinical diagnostics, and environmental monitoring, as well as in applications such as the determination of heavy metals and inorganic anions and pesticide analysis [40, 41]. Nanomaterials such as metal nanoparticles (AuNPs, AgNPs), carbon nanotubes (CNTs, MWCNTs), graphene, and conducting polymers are used in the development of new electrochemical sensor platforms owing to their unique chemical, electronic and mechanical properties compared to conventional materials [38, 42].

Recently, to fabricate new biosensors, conducting polymers such as poly(5-amino-2-mercapto-1,3,4-thiadiazole), polypyrrole, poly(3,4-ethylene dioxythiophene), and polyaniline have received considerable attention in the scientific and technological fields owing to their biological, chemical, thermal, optical, and electrical properties [43, 44]. Electrochemical sensors and biosensors based on conductive polymers play a significant role in public health and environmental protection due to their several merits such as easy preparation, rapid detection, high sensitivity, and small size [45]. Among different nanocomposite materials, the production of conductive polymers containing AuNPs has received considerable attention due to their superior optical and electrocatalytic properties [46]. AuNPs have received much interest in pesticide detection due to their remarkable characteristics improving the analytical sensitivity of biosensors [47]. AuNPs, the most stable nanoparticles, have unique advantages including desirable biocompatibility, magnetic properties, and efficient electron transfer [48]. Thus, AuNPs are mostly used as the immobilization matrix in biosensors systems to enhance the performance of biosensors [11]. The amount of the immobilized aptamer on the electrode surface greatly affects the accuracy and sensitivity of aptasensors [49]. According to earlier literature reports, nanostructured materials having large surface area and many binding sites were used to design aptasensing platforms, such as AuNPs [50] and CNTs [51], which were required to enhance the amount of immobilized aptamer and to amplify the detection signals of the electrochemical system.

Highlights

- A novel sandwich-type aptasensor based on SPE/P(AMT)/AuNPs was constructed.
- SEM, XPS, CV, and EIS were employed to characterize the modified electrodes.
- The proposed aptasensor demonstrated good reproducibility, selectivity, and sensitivity.
- The sensing strategy was successfully used to test ACE in real samples with high recovery values.

Herein, an aptamer-based electrochemical biosensor based on a sandwich hybridization for ACE detection, was proposed using the poly-5-amino-2-mercapto-1,3,4-thiadiazole [P(AMT)]/gold nanoparticles (AuNPs)-modified screen-printed electrode (SPE). The morphological, spectroscopic, and electrochemical characterizations of the developed electrodes were also investigated. Several experimental parameters, such as aptamer sequences, incubation time, and aptamer concentrations were optimized. The proposed aptasensor exhibited good analytical performances such as very low detection limit, wide linear range, and low RSD for the ACE detection. Additionally, the fabricated sensor was tested using real samples to demonstrate the sensitivity of the assay.

2. Experimental

2.1. Chemicals and apparatus

Sulfuric acid (H_2SO_4), AMT, bovine serum albumin (BSA), diethanolamine (DEA), potassium ferro-ferricyanide ($K_4Fe(CN)_6/K_3Fe(CN)_6$), disodium hydrogen phosphate dihydrate ($Na_2HPO_4 \cdot 2H_2O$), monosodium dihydrogen phosphate dihydrate ($NaH_2PO_4 \cdot 2H_2O$), 1-naphthyl phosphate, 6-mercapto-1-hexanol, ACE, atrazine, omethoate, imidacloprid, chlorpyrifos, and streptavidin–alkaline phosphatase (strep–ALP) conjugate were purchased from Aldrich (Sigma–Aldrich Co., Germany) and hydrogen tetrachloroaurate trihydrate (($HAuCl_4) \cdot 3H_2O$) was supplied from Acros Organics ().

Aptamers were selected according to the previous literature [52]. The synthetic oligonucleotides used were supplied from Eurofins Genomics (Ebersberg, Germany) with the following sequences:

Aptamer 1 = S10THIOL:(5′-(SH)-ATTGGACTAGCTGCAGCGATTCTTAATCGCTATGCTCCGCCCAATACTG-3′)

Aptamer 1 (Chosen) = S18THIOL:(5′-(SH)-TGTAATTTGTCTGCAGCGGTTCTTGATCGCTGACACCATATTATGAAGA-3′)

Aptamer 2 = S10BIO:(5′-(BIO)-ATTGGACTAGCTGCAGCGATTCTTAATCGCTATGCTCCGCCCAAT-3′)

Phosphate buffer solution (PBS, 0.5 mol L^{-1}, pH 7.5) as supporting electrolyte was prepared by dissolving the required amount of NaH_2PO_4 and Na_2HPO_4 into ultrapure water. Aptamer stock solutions were prepared with 0.5 mol L^{-1} PBS and stored at −18 °C.

Stock S10 and S18 aptamer solutions were prepared in 0.5 mol L^{-1} pH 7.5 PBS as 29.8 and 21.0 μmol L^{-1}, respectively. Aptamer solutions ranging from 0.5 to 5.0 μmol L^{-1} were prepared by using the stock solutions. TRIS–HCl buffer solution (20 mmol L^{-1}; pH 7.4) was prepared by mixing 0.1 mol L^{-1} NaOH, 0.2 mol L^{-1} KCl, and 5.0 mmol L^{-1} $MgCl_2$ and adjusted the pH with 0.1 mol L^{-1} NaOH and HCl solutions. AMT monomer (1.37 mg) was weighed and dissolved in 0.1 M H_2SO_4 under nitrogen gas for 30 Min. To prepare DEA buffer solution (0.1 mol L^{-1}, pH 9.6), 0.1 mol L^{-1} DEA, 1.0 mmol L^{-1} $MgCl_2$, and 0.1 mol L^{-1} KCl were mixed and the pH was adjusted to 9.6. The strep–ALP conjugate was dissolved in 2 mL of DEA buffer (1,639 U/1.0 mL). The BSA–enzyme mixture was prepared with DEA buffer containing 8.0 mg/mL BSA and 1.0 U/mL strep–ALP enzyme, respectively. α-Naphthyl phosphate solution was prepared by dissolving 1.0 mg of α-naphthyl phosphate in 1.0 mL of DEA buffer. $HAuCl_4 \cdot 3H_2O$ solution (0.6 mmol L^{-1}) was prepared by using the stock $HAuCl_4 \cdot 3H_2O$ solution (50 mmol L^{-1}) and dissolved in H_2SO_4.

All electrochemical experiments were performed at room temperature by using an electrochemical workstation (AUTOLAB-PGSTAT 302N with FRA 2.0 module and Nova 1. 11 software). For the analysis of the impedance plots, a sinus wave of 5 mV amplitude was selected in the frequency range of 100 kHz and 0.01 Hz to the SPE/modified SPE.

SPEs (Dropsens; DRP-C110, Oviedo, Spain) were used as the working electrode. A 60 μL droplet covered the working area was placed for measurements onto SPEs.

2.2. Preparation and characterization of modified electrodes

P(AMT) film onto the SPE surface was synthesized by the procedure as reported in the literature [53]. Briefly, the SPE electrode was incubated in 0.1 mol L^{-1} H_2SO_4 solution containing 1.0 mmol L^{-1} AMT and cyclic voltammetry (CV) was performed on the surface of SPE in the potential range from −0.20 to +1.70 V at a scan rate of 50 mV Sec^{-1} (15 scans). Then P(AMT)-modified SPE (SPE/P(AMT)) electrode was rinsed with double-distilled water thoroughly and allowed to dry in the air. The AuNPs were electrochemically deposited onto the SPE/P(AMT) by the voltammetric method in 0.1 mol L^{-1} H_2SO_4 solution that contains 0.6 mmol L^{-1} $HAuCl_4$ solution using CV technique and 25 successive potential sweeps were applied between −0.20 and +1.20 V at a scan rate of 100 mV Sec^{1}. The obtained SPE/P(AMT)/AuNPs electrodes were washed with ultrapure water and allowed to dry at room temperature.

Electrochemical characterizations of bare SPE, SPE/P(AMT), SPE/AuNPs, and SPE/P(AMT)/AuNPs electrodes were carried out by CV and electrochemical impedance spectroscopy (EIS) techniques in 1.0 mol L^{-1} KCl solution containing 5.0 mol L^{-1} $Fe(CN)_6^{3-/4-}$. The morphologies of the prepared electrodes were examined using a field-emission scanning electron microscope (FEI Nova NanoSEM 650; FEI, The Netherlands). X-ray photoelectron spectra were recorded using a PHI 5000 Versa Probe spectrometer (Physical Electronics, USA).

2.3. Aptasensor development and ACE detection

For the fabrication of aptasensor (Scheme 1), 60 μL of Apt1 solution solutions was dropped onto the SPE/P(AMT)/AuNPs electrodes and it was allowed to provide chemisorption proceed overnight (∼16 H) at +4 °C. The obtained electrodes were stored in Petri dishes to keep the solutions from evaporation. After the immobilization of Apt 1, sensors were interacted with 6-mercaptohexanol for 60 Min to remove the nonspecific interactions and washed with pH 7.4 TRIS–HCl buffer solution. Then, ACE solutions in the range of 5×10^{-12}–1×10^{-9} mol L^{-1} concentration were dropped on the

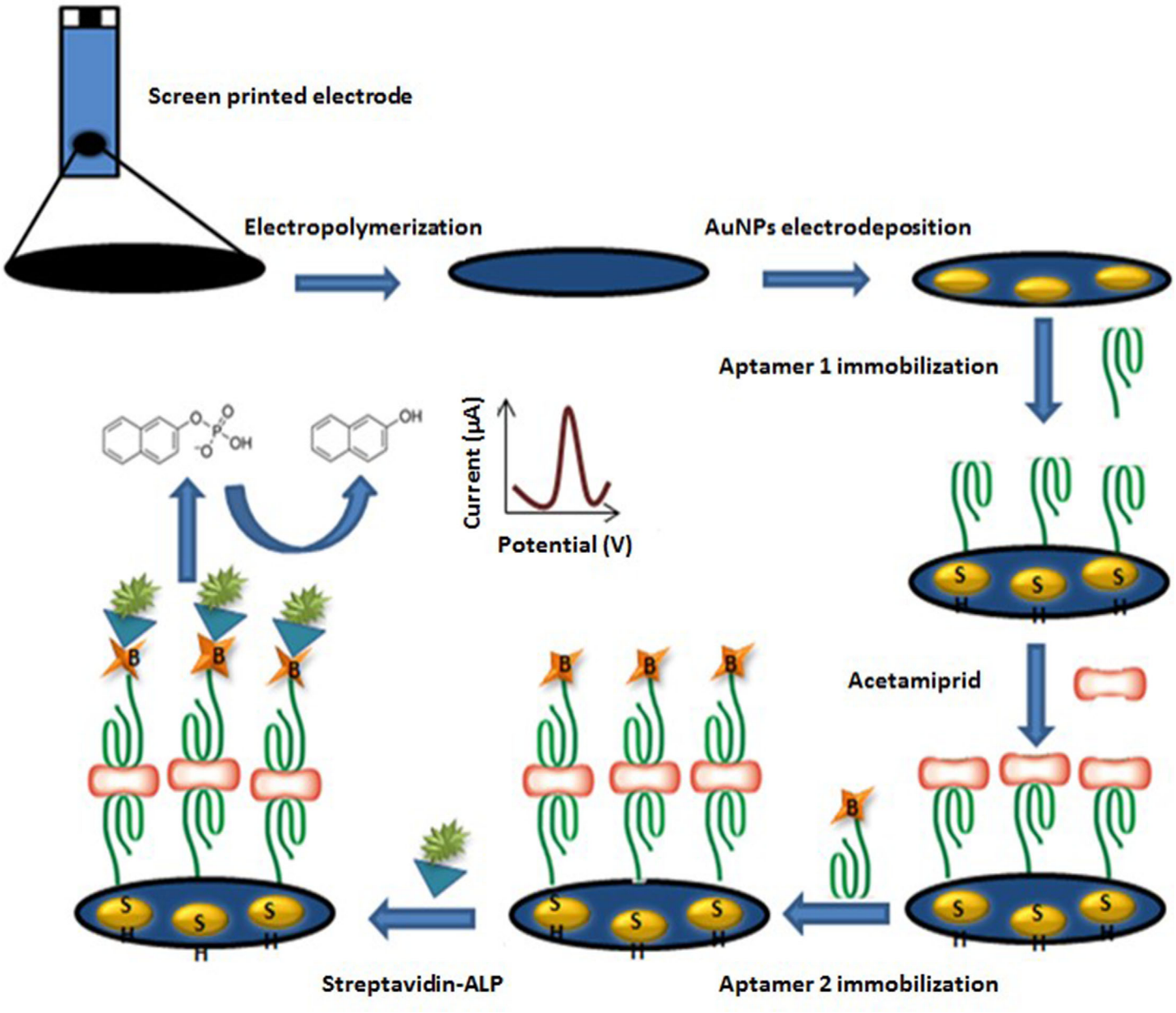

SCHEME 1 *Fabrication steps of the proposed aptasensor.*

prepared SPE/P(AMT)/AuNPs/Apt1 electrodes. After 45 Min, the aptasensors were washed with TRIS–HCl buffer. Then, the biotin-labeled Apt2 solution was dropped on the electrode surface and allowed to interact for 20 Min. Then, the enzyme-labeled step was performed. In this step, the aptasensors were interacted strep–ALP conjugate solution containing (1.0 U/mL) 8.0 mg/mL BSA (DEA buffer, 0.1 mol L^{-1} pH 9.6). After 20 Min, the aptasensors were washed with DEA buffer. Finally, 60 μL of a solution 1.0 mg/mL of the enzymatic substrate α-naphthyl-phosphate in DEA buffer interacted with the aptasensor and the determination of ACE was performed by using the electro-oxidation signal of α-naphthol, which is an obtained product from the interaction between ALP and α-naphthyl phosphate. The enzymatic product α-naphthol was used as an electroactive substance and it was detected by DPV.

2.4. Real sample analysis

Using the developed SPE/P(AMT)/AuNPs/Apt1/ACE/Apt2 electrode, the standard addition method was used to determine the ACE in real samples. Pesticide samples containing ACE are provided from Hacettepe University. The amount of ACE in these samples was previously determined by the HPLC method and it was found to be 10%. ACE was determined by the developed aptasensor, which was prepared by using ACE

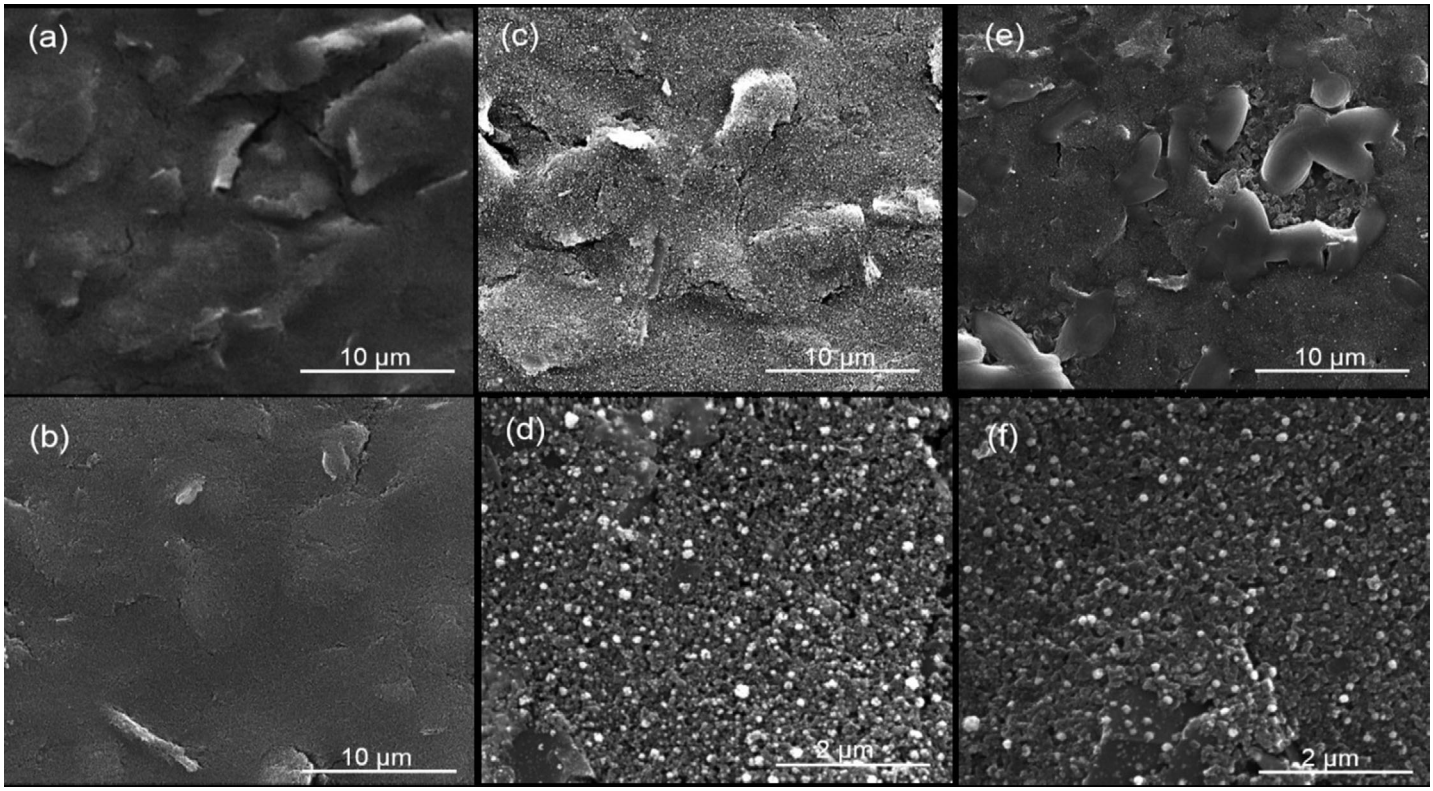

FIG. 1 *SEM micrographs of the bare SPE (A), SPE/P(AMT) (B), SPE/P(AMT)/AuNPs (C and D), SPE/P(AMT)/AuNPs/Apt1 (E and F).*

samples at certain concentrations. By comparing the results between the two methods, the applicability of the developed method has been tested. The applicability of the method was also investigated with samples of wastewater, tomatoes, and cucumbers. Cucumber (100 g) and 100 g of tomato were placed separately in 100 mL phosphate buffer (0.05 mol L^{-1}, pH 7.5) and homogenized with a blender and then filtered. Then, the samples were centrifuged at 2800 *g* and the supernatants were used as samples. Tap water was used as an example of wastewater. Certain amounts of ACE solutions were added to wastewater, tomato, and cucumber samples by standard addition method and the amount of ACE in samples was detected by using the developed aptasensor. Recovery % and RSD % values were calculated for each sample using the results obtained.

3. Results and Discussion

3.1. Characterization of modified screen-printed carbon electrodes

Ferro-ferricyanide ion ($Fe(CN)_6^{3-/4-}$) was mostly used as a redox probe to examine the electron transfer features of nanomaterial modified electrodes [54]. Figure S1 shows the cyclic voltammograms of the bare and modified SPEs. When P(AMT) was coated on the bare SPE surface, it was observed that the anodic and cathodic peak currents of $Fe(CN)_6^{3-/4-}$ redox probe increased and the peak–peak separation value (ΔE_p) decreased (Fig. S1c). It can be concluded that P(AMT) film significantly improves the redox reaction and increases the electroactive surface area of the polymer film [55]. It was observed that the anodic and cathodic current values (ip_a and ip_c) were higher than those of the SPE/P(AMT) electrode when the bare SPE surface was coated with AuNPs (Fig. S1b). The results showed that the AuNPs deposited on the SPE surface increased the electrode performance by accelerating the electron transfer rate at the electrode/solution interface [11]. After the electrodeposition of AuNPs on the SPE/P(AMT) electrode, the highest current values were obtained due to the conductivity of a new nanocomposite containing conducting polymer and metallic nanoparticle. (Fig. S1d). ΔE_p, ip_a, and ip_c values of bare SPE, SPE/P(AMT), SPE/AuNPs, and SPE/P(AMT)/AuNPs electrodes are shown in Table S1.

Electron transfer properties of SPE, SPE/P(AMT), and SPE/P(AMT)/AuNPs electrodes were also examined by the EIS method and Nyquist curves obtained were shown in Fig. S2. A typical Nyquist curve shows a semicircle portion at high frequencies, which refers to the electron transfer limited process, and a linear portion at lower frequencies, which corresponds to the diffusion process. The diameter of the semicircle is equal to the electron or charge transfer resistance (R_{et}) [43]. The values of SPE, SPE/P(AMT) SPE/AuNPs, and SPE/P(AMT)/AuNPs electrodes were found as 609, 173, 75.7, and 34.1 Ω, respectively. Compared with the bare SPE electrode (Fig. S2a), the lower R_{et} values obtained from SPE/P(AMT) (Fig. S2b) and SPE/AuNPs (Fig. S2c) electrodes show that the electron

transfer rate at the interface is enhanced. With the synergistic effect between P(AMT) film and AuNPs, it is seen that the R_{et} value between electrode interface and $Fe(CN)_6^{3-/4-}$ is the lowest compared with other modified electrodes (Fig. S2d).

The change in surface morphology was monitored by SEM and the results are exhibited in Fig. 1. When the SEM images of the bare SPE (Fig. 1A) and SPE/P(AMT) (Fig. 1B) are examined, it is seen that P(AMT) is coated on the SPE surface by creating a thin film and decreasing the surface porosity of the bare SPE. After the electrodeposition of AuNPs on the surface of the SPE/P(AMT), it can be seen in Figs. 1C and 1D that the nano-sized AuNPs are homogeneously distributed on the surface of the polymer film. The presence of AuNPs on the SPE/P(AMT) surface led to an increase in the surface area and enhance the electrochemical sensitivity [56]. After the Apt1 immobilization on the SPE/P(AMT)/AuNPs surface, it was observed that the cavities between the AuNPs were removed and covered with Apt1 (Figs. 1E and 1F).

X-ray photoelectron spectroscopy (XPS) is the most widely used method for the analysis and surface characterization of elements, inorganic combinations, biomedical materials, and polymers as a wide range of materials can be used and can provide valuable quantitative and chemical information from the surface of the material [57]. XPS measurements were carried out to determine the P(AMT) and AuNPs accumulated on the surface of the prepared electrodes and the results are given in Fig. 2. In Fig. 2A, when the survey spectra of SPE (a), SPE/P(AMT) (b), and SPE/P(AMT)/AuNPs (c) electrodes are examined, the bare SPE has only C1s, O1s, and OKLL peaks. It is reported that the presence of O1s peak in the bare SPE may be caused by the preparation and storage procedure [58]. The appearance of S2p and N1s peaks in addition to these peaks on the SPE/P(AMT) electrode indicates the presence of the polymer in the structure (Fig. 2A(b)). After the electrodeposition of AuNPs on the P(AMT) coated electrode, the peaks of Au are also observed (Fig. 2A(c)). In the expanded XPS spectra, two different peaks corresponding to N1s are seen (Fig. 2B). These peaks were assigned to be –N = (397.6 eV) and –NH– (399.4 eV), respectively. When the XPS spectrum of S2p was examined, –S–C– bond in the aromatic ring was observed at 165.2 eV, whereas the peak of the disulfide bond obtained after polymerization was obtained at 163.5 eV (Fig. 2C). The results suggested that the SPE surface was successfully coated with AuNPs and P(AMT) [59].

3.2. The optimization of experimental conditions

It is significant to choose the optimal parameters involved in the process of aptasensor construction and ACE detection to develop a highly sensitive method with a low detection limit. First, the influence of the sequence and amount of Apt1 on the EIS responses of SPE/P(AMT)/AuNPs was investigated by using two different ACE binding DNA aptamers (S10 and S18) with the aptamer concentrations range of 0.5–5.0 μmol L^{-1}. As shown in Fig. 3A, the R_{et} values of the S18 were higher than

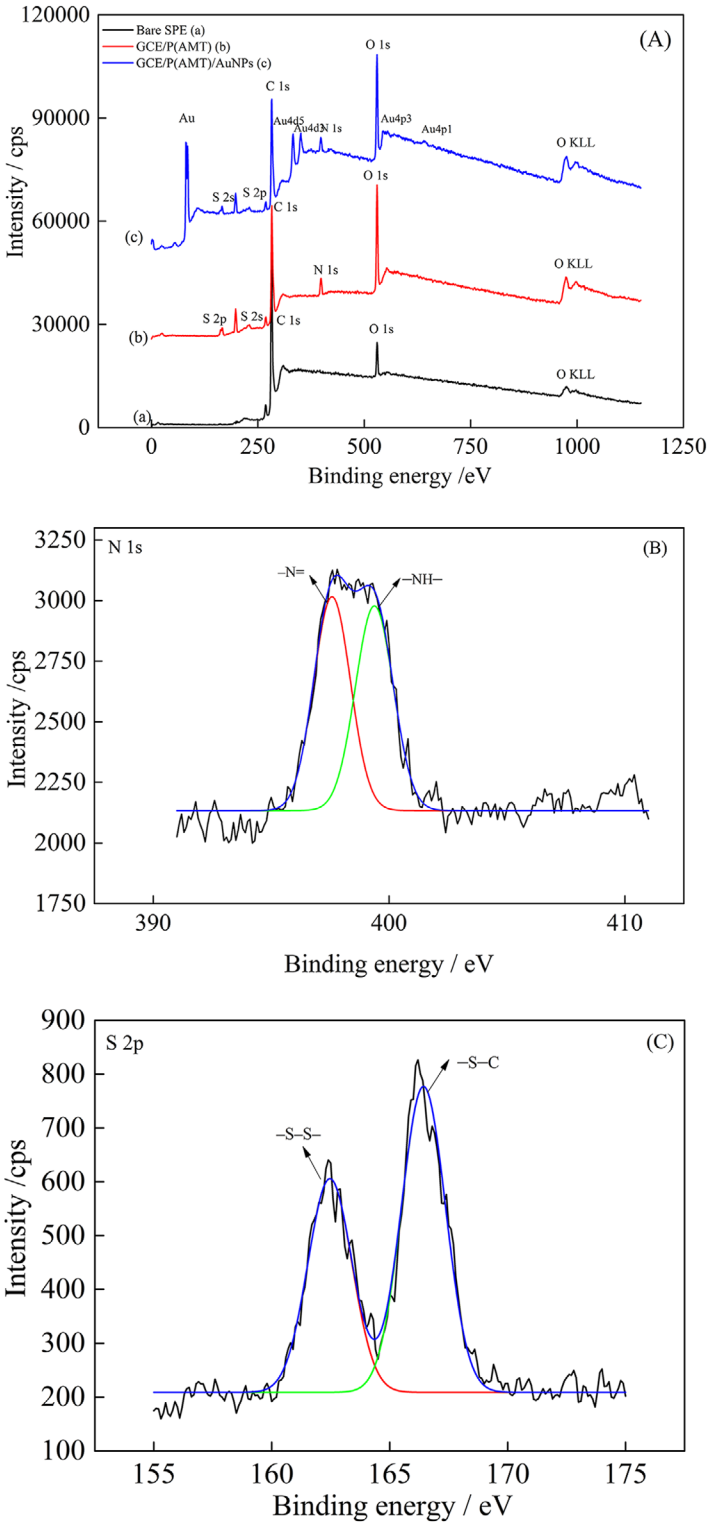

FIG. 2 *(A) XPS spectra of the bare SPE (a), SPE/P(AMT) (b), SPE/P(AMT)/AuNPs (c) electrodes, extended XPS for (B) N1s and (C) S2p on SPE/P(AMT)/AuNPs electrode.*

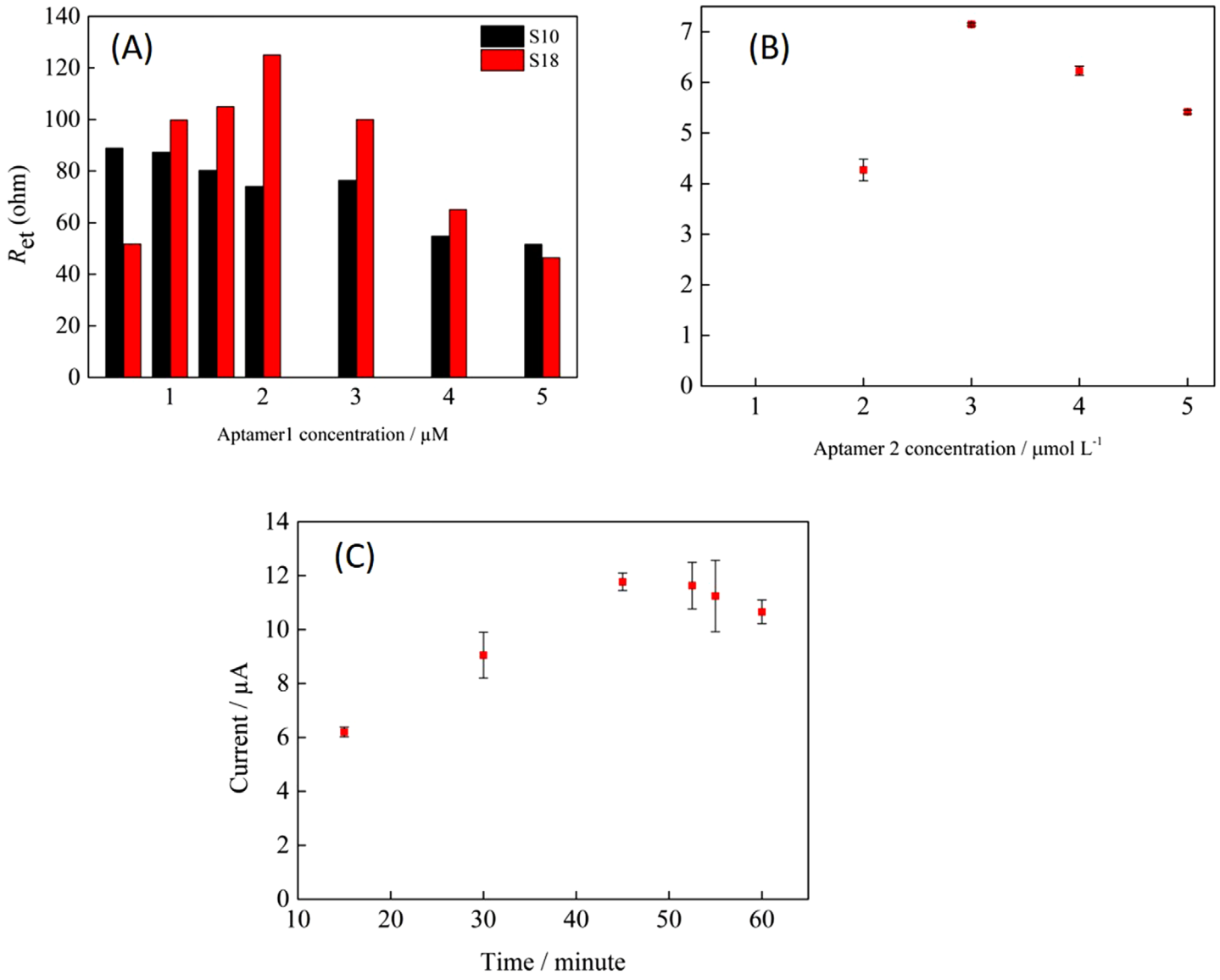

FIG. 3 *(A) The effect of the sequence and concentration of aptamer on the EIS response. (B) The effect of Apt 2 concentration on DPV signal of α-naphthol. (C) The effect of immobilization time on DPV signal of α-naphthol.*

that of the S10 and increased up to 2.0 μmol L^{-1}. The results indicated that the S18 aptamer has more ability to bind to the SPE/P(AMT)/AuNPs surface. Thus, Apt1 concentration and sequence were selected as 2.0 μmol L^{-1} and S18, respectively. Then, the concentration of the biotin-labeled second aptamer (Apt2, S10-BIO) was optimized. Figure 3B exhibits the oxidation currents of α-naphthol changed with the Apt2 concentration in the range of 2.0 and 5.0 μmol L^{-1}. As shown in Fig. 3B, the oxidation currents of α-naphthol reached to the maximum value at 3.0 μmol L^{-1}. However, with a further increase in aptamer concentration, the current response decreased due to the saturation behavior of the increased amount of aptamer. Thus, 3.0 μmol L^{-1} was determined as optimum Apt2 concentration. The highest peak currents of α-naphthol were obtained by using S18 and S10 sequences at the concentrations of 2.0 and 3.0 μmol L^{-1}, respectively. In other words, the aptamer S18 and S10 may possess different binding sites toward ACE allowing the surface sandwich assay with aptamer S18 as a capture probe and S10 as a target probe for the ACE pesticide. After that, the interaction time between ACE and SPE/P(AMT)/AuNPs/Apt1 electrode was studied. By keeping the constant amount of ACE, the SPE/P(AMT)/AuNPs/Apt1 electrode interacted with ACE at certain times (15; 30; 45; 52,5; 55; and 60 Min) and the optimum interaction time was determined. As shown in Fig. 3C, the peak current of ACE increased up to 45 Min with the time and thereafter remained nearly constant. Thus, optimum interaction time was selected as 45 Min and used in all subsequent experiments.

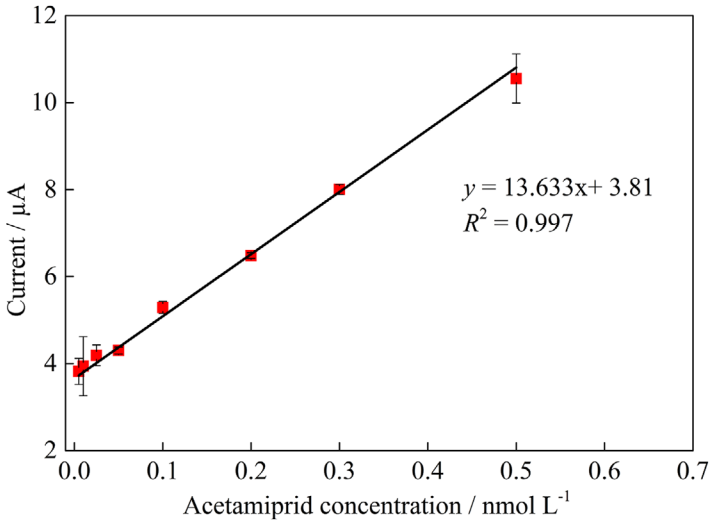

FIG. 4 *The effect of ACE concentration on the DPV signal of α-naphthol*

3.3. Analytical performance of the developed aptasensor

The electrochemical determination of ACE was carried out using solutions at different concentrations. Under the optimal experimental conditions, the DPV responses of the developed aptasensor for the detection of ACE with different concentrations were obtained. As can be seen from Fig. 4, a linear dependence was observed in the concentration range of 5.0×10^{-12}–5.0×10^{-10} mol L^{-1} ACE ($R^2 = 0.997$). The limit of detection (LOD) and the limit of quantification (LOQ) values confirmed the sensitivity of the modified electrode, which is calculated using the following equation [58]. The LOD and the LOQ values were found to be 1.5 and 5.0 pmol L^{-1}, respectively.

$$\mathrm{LOD} = 3s/m$$

$$\mathrm{LOD} = 10s/m$$

where s is the standard deviation of the current of the lowest concentration of the linearity range, m is the slope of the related calibration curve [60]. Compared to the other published methods, this developed aptasensor has a wider linear range with high sensitivity and much lower LOD than the reported strategies [10, 11, 13, 31, 49, 61-67] (Table 1). Hence, our developed aptasensor provides an alternative approach due to its high sensitivity and ease of operation.

3.4. Interferences and reproducibility

To investigate the selectivity of the developed aptasensor, the effect of some interfering pesticides such as atrazine, omethoate, imidacloprid, and chlorpyrifos pesticides were examined. For this purpose, the solutions of atrazine, omethoate, imidacloprid, and chlorpyrifos were each prepared to have a concentration of 0.05 nmol L^{-1}. The prepared aptasensor was interacted with the solutions containing each of the pesticide and ACE (0.05 nmol L^{-1}). The α-naphthol oxidation signal obtained after the interaction was measured and compared with the result

TABLE 1 ***A comparison of different methods of acetamiprid detection with the current study***

Method	*Linear range (mol L^{-1})*	*LOD (mol L^{-1})*	*References*
Disposable electrochemical DNA aptasensor	2.5×10^{-7}–2.0×10^{-6}	8.6×10^{-8}	[13]
Chemiluminescence aptasensor	8.0–63.0×10^{-8}	6.2×10^{-7}	[61]
EIS-based aptasensor	5.0×10^{-14}–1.0×10^{-5}	1.7×10^{-14}	[49]
AuNPs-modified electrode	5.0×10^{-9}–6.0×10^{-7}	1.0×10^{-9}	[11]
Electrochemical aptamer-based assay	5.0×10^{-10}–6.5×10^{-7}	1.53×10^{-14}	[62]
A fluorometric aptamer-based assay	5.0×10^{-9}–5.0×10^{-8}	2.8×10^{-9}	[63]
SERS-based aptasensor	3.0×10^{-8}–4.0×10^{-6}	1.76×10^{-8}	[64]
A label-free and enzyme-free fluorescent aptasensor	5.0×10^{-9}–5.0×10^{-7}	2.37×10^{-9}	[65]
Triple-helix molecular switch (THMS)	1.0×10^{-7}–1.2×10^{-6}	9.12×10^{-9}	[10]
Turn-on sensor based on quantum dots	0–1.5×10^{-7}	0.7×10^{-9}	[66]
AgNPs anchored on nitrogen-doped graphene	1.0×10^{-13}–5.0×10^{-9}	3.3×10^{-14}	[67]
Fluorometric label-free aptasensor	1.6×10^{-9}–1.2×10^{-7}	0.3×10^{-9}	[31]
Aptamer-based electrochemical biosensor based on sandwich hybridization	5.0×10^{-12}–5.0×10^{-10}	1.5×10^{-12}	This study

TABLE 2 *The interference effect of other species on the developed aptasensor for ACE determination*

Interference	*Concentration (nmol L^{-1})*	*Interference%*
Atrazine	0.05	−0.52
Omethoate	0.05	0.84
Imidacloprid	0.05	−6.65
Chlorpyrifos	0.05	−4.52

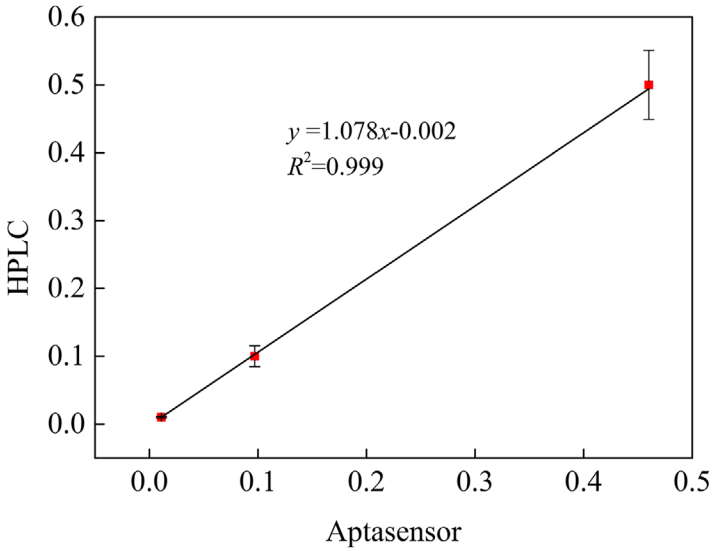

FIG. 5 *Compatibility of the methods in pesticide samples for ACE determination*

obtained from the solution containing ACE and % interference values for each pesticide were calculated according to the following formula;

$$Interference\% = [(I_x - I_0)/I_0] \times 100$$

I_x, DPV signal of 0.05 nmol L^{-1} interference and 0.05 nmol L^{-1} ACE solution; I_0, DPV signal of 0.05 nmol L^{-1} ACE solution.

As shown in Table 2, it can be concluded that the interference effect of each species is quite low and has a negligible effect on the ACE determination.

The usability of biosensors in routine analyses is related to whether they can be reproduced correctly, reliably, and at the same standard. Therefore, one of the most important characteristic features to be examined after developing a new biosensor is the reproducibility of that biosensor. To investigate the reproducibility of the aptasensor, seven independent aptasensors were prepared and tested using 0.05 nmol L^{-1} of ACE at the proposed aptasensor. The RSD values of the DPV peak currents of α-naphthol was calculated as 7.00%. The reproducibility of this aptasensor is below 10% and allows a fast and sensitive determination of ACE.

3.5. Application of aptasensor to real sample analysis

To test the applicability of the proposed aptasensor in the practical analysis, the pesticide samples containing ACE were supplied from Hacettepe University Pesticide Research and Reference Laboratory and tested with the developed aptasensor. The results are exhibited in Fig. 5 and these show that the determination of ACE using the fabricated aptasensor can be performed successfully without the influence of some interfering species found in pesticide samples. The t values for different ACE concentrations were calculated as 1.18, 1.40, and 1.72 at 95% confidence level ($t_{critic,}$ 2.13). The DPV results of the developed aptasensor are in accordance with the results obtained from the HPLC method.

To demonstrate the applicability of the developed aptasensor in practical analysis, it was used to detect ACE in wastewater, tomatoes, and cucumbers. The recoveries were calculated for the sample solutions by the standard addition method. The results were shown in Table 3. The recoveries are in the range from 99.6% to 106.0% with RSD values (0.05%–10.36%) (n = 3). The results suggest that the proposed aptasensor provided a new electrochemical sensing approach for the determination of ACE in food samples and environmental residues. There are some reported studies in the literature with recovery values of 93.8%–105.0% [60], 90.4%–114.0% [10], and 100.68%–112.8% [68].

4. Conclusions

In this study, an aptamer-based electrochemical biosensor based on sandwich hybridization was developed for the rapid, reliable, and sensitive determination of an important insecticide, ACE. Compared with the traditional pesticide sensing strategies, highlights of this work are summarized as follows: (i) use of AuNPs and P(AMT) can efficiently increase the surface area of the electrode, thus resulting in the electrochemical signal amplification; (ii) introduction of highly specific aptamers can significantly enhance the sensitivity, and (iii) the obtained sandwich-based sensing system can block the unspecific interactions, increasing the selectivity. The proposed aptasensor exhibited good selectivity, reproducibility, high sensitivity with a wide linear range (5×10^{-12}–5×10^{-10} mol L^{-1}), and low detection limit (1.5 pmol L^{-1}) for the ACE detection. The new sensing strategy also has several advantages such as simple, fast, and low cost compared with the traditional methods such as HPLC, GC–MS, and ELISA, which are widely used in pesticide analysis. Nevertheless, one major disadvantage of using the SPE/P(AMT)/AuNPs/Apt1/ACE/Apt2 sensing strategy is the long incubation time for the reaction of the Apt1. Thus, future work should be focused on the improvement of the incubation time. Furthermore, it can be understood that the developed aptamer-based sandwich method can be used for the sensitive

TABLE 3 *Results of real sample analysis with different ACE concentrations*

Sample	*Added (nmol L^{-1})*	*Detected (nmol L^{-1})*	*Recovery (%)*	*RSD[a] (%)*
Waste water	0.0050	0.0049	99.6	4.69
	0.0500	0.0510	102.0	10.36
Tomato	0.0050	0.0052	104.0	4.45
	0.0100	0.0106	106.0	2.04
	0.1000	0.1042	104.2	0.05
Cucumber	0.0100	0.0101	101.0	3.76
	0.1000	0.1040	104.0	1.06

[a]The results have been given average of three measurements.

and selective determination of other pesticide species in real samples at nanomolar levels.

5. Acknowledgements

This study is produced from MSc thesis of Mustafa Barış Koçer (Ankara University Graduate School of Natural and Applied Sciences) and supported by the Scientific and Technological Research Council of Turkey (TUBITAK grant no. 214Z203).

6. References

[1] Goulson, D. (2013) J. Appl. Ecol. 50, 977–987.
[2] Ma, X., Li, H., Xiong, J., Mehler, W. T., and You, J. (2019) J. Agric. Food Chem. 67, 2429–2436.
[3] Tian, Y., Wang, Y., Sheng, Z., Li, T., and Li, X. (2016) Anal. Biochem. 513, 87–92.
[4] Shirani, M. P., Rezaei, B., and Ensafi, A. A. (2019) Spectrochim. Acta Part A 210, 36–43.
[5] Abdel-Ghany, M. F., Hussein, L. A., and El Azab, N. F. (2017) J. AOAC Int. 100, 176–188.
[6] Purohit, P., and Malik, S.. Isolation and characterization of acetamiprid – A neonicotinoid insecticide using TLC and GC-mass spectrometry. AIP Publishing LLC, pp. 080018.
[7] López-Fernández, O., Rial-Otero, R., and Simal-Gándara, J. (2015) Anal. Bioanal. Chem. 407, 7101–7110.
[8] Lee, H. S., Kim, S.-W., Abd El-Aty, A., Chung, H. S., Kabir, M. H., Rahman, M. M., Jeong, J. H., Chang, B.-J., Shin, H.-C., and Shim, J.-H. (2017) J. Chromatogr. B 1055, 172–177.
[9] Watanabe, E., Yamasaki, T., Hirakawa, Y., Harada, A., Iwasa, S., and Miyake, S. (2018) Anal. Methods 10, 3162–3169.
[10] Liu, X., Li, Y., Liang, J., Zhu, W., Xu, J., Su, R., Yuan, L., and Sun, C. (2016) Talanta 160, 99–105.
[11] Fan, L., Zhao, G., Shi, H., Liu, M., and Li, Z. (2013) Biosens. Bioelectron. 43, 12–18.
[12] Verma, N., and Bhardwaj, A. (2015) Appl. Biochem. Biotechnol. 175, 3093–3119.
[13] Rapini, R., Cincinelli, A., and Marrazza, G. (2016) Talanta 161, 15–21.
[14] Ali, M. H., Elsherbiny, M. E., and Emara, M. (2019) Int. J. Mol. Sci. 20, 2511.
[15] Zhang, Y., Lai, B. S., and Juhas, M. (2019) Molecules 24, 941.
[16] Ellington, A. D., and Szostak, J. W. (1990) Nature 346, 818.
[17] Mascini, M. (2008) Anal. Bioanal. Chem. 390, 987–988.
[18] Zhan, Y., Tang, J., Huang, D., Zou, L., and Ye, B. (2019) Talanta 198, 302–309.
[19] Li, Y., Ran, G., Lu, G., Ni, X., Liu, D., Sun, J., Xie, C., Yao, D., and Bai, W. (2019) J. Electrochem. Soc. 166, B449.
[20] Qi, X., Yan, X., Zhao, L., Huang, Y., Wang, S., and Liang, X. (2020) J. Electroanal. Chem. 858, 113805.
[21] Mishra, G. K., Sharma, V., and Mishra, R. K. (2018) Biosensors 8, 28.
[22] Zhou, W., Huang, P.-J. J., Ding, J., and Liu, J. (2014) Analyst 139, 2627–2640.
[23] Qiu, Z., Shu, J., Liu, J., and Tang, D. (2018) Anal. Chem. 91, 1260–1268.
[24] Lv, S., Zhang, K., Zhu, L., and Tang, D. (2019) Anal. Chem. 92, 1470–1476.
[25] Razmi, N., Baradaran, B., Hejazi, M., Hasanzadeh, M., Mosafer, J., Mokhtarzadeh, A., and de la Guardia, M. (2018) Biosens. Bioelectron. 113, 58–71.
[26] Wang, Y., Zhao, G., Zhang, Q., Wang, H., Zhang, Y., Cao, W., Zhang, N., Du, B., and Wei, Q. (2019) Sens. Actuators B 288, 325–331.
[27] Wu, S., Yu, Q., He, C., and Duan, N. (2020) Spectrochim. Acta Part A 224, 117387.
[28] Schoukroun-Barnes, L. R., Wagan, S., and White, R. J. (2014) Anal. Chem. 86, 1131–1137.
[29] Blidar, A., Feier, B., Tertis, M., Galatus, R., and Cristea, C. (2019) Anal. Bioanal. Chem. 411, 1053–1065.
[30] Rapini, R., and Marrazza, G. (2017) Bioelectrochemistry 118, 47–61.
[31] Saberi, Z., Rezaei, B., and Ensafi, A. A. (2019) Microchim. Acta 186, 273.
[32] Fu, J., An, X., Yao, Y., Guo, Y., and Sun, X. (2019) Sens. Actuators B 287, 503–509.
[33] Vasilescu, A., Hayat, A., Gáspár, S., and Marty, J. L. (2018) Electroanalysis 30, 2–19.
[34] Liu, M., Khan, A., Wang, Z., Liu, Y., Yang, G., Deng, Y., and He, N. (2019) Biosens. Bioelectron. 130, 174–184.
[35] McKeague, M., Giamberardino, A., and DeRosa, M. C., (2011) Advances in Aptamer-Based Biosensors for Food Safety. London: IntechOpen.
[36] Das, R., Dhiman, A., Mishra, S. K., Haldar, S., Sharma, N., Bansal, A., Ahmad, Y., Kumar, A., Tyagi, J. S., and Sharma, T. K. (2019) Int. J. Nanomed. 14, 2103.
[37] Ghosh, S., Datta, D., Cheema, M., Dutta, M., and Stroscio, M. A. (2017) Nanotechnology 28, 435505.
[38] Marín, S., and Merkoçi, A. (2012) Electroanalysis 24, 459–469.
[39] Govindhan, M., Adhikari, B.-R., and Chen, A. (2014) RSC Adv. 4, 63741–63760.
[40] Maduraiveeran, G., and Jin, W. (2017) Trends Environ. Anal. Chem. 13, 10–23.
[41] Ding, Y., Wang, S., Li, J., and Chen, L. (2016) TrAC Trends Anal. Chem. 82, 175–190.
[42] Murtada, K., and Moreno, V. (2020) J. Electroanal. Chem. 113988.
[43] Aydoğdu, G., Günendi, G., Zeybek, D. K., Zeybek, B., and Pekyardımcı, Ş. (2014) Sens. Actuators B 197, 211–219.
[44] Shafaat, A., Faridbod, F., and Ganjali, M. R. (2018) New J. Chem. 42, 6034–6039.

[45] John, B. (2020) Polymer Nanocomposite-Based Electrochemical Sensors and Biosensors. London: , IntechOpen.
[46] Naseri, M., Fotouhi, L., and Ehsani, A. (2018) Chem. Rec. 18, 599–618.
[47] Dou, X., Chu, X., Kong, W., Luo, J., and Yang, M. (2015) Anal. Chim. Acta 891, 291–297.
[48] Xiong, S., Deng, Y., Zhou, Y., Gong, D., Xu, Y., Yang, L., Chen, H., Chen, L., Song, T., and Luo, A. (2018) Anal. Methods 10, 5468–5479.
[49] Fei, A., Liu, Q., Huan, J., Qian, J., Dong, X., Qiu, B., Mao, H., and Wang, K. (2015) Biosens. Bioelectron. 70, 122–129.
[50] Li, Y., Qi, H., Peng, Y., Yang, J., and Zhang, C. (2007) Electrochem. Commun. 9, 2571–2575.
[51] Zelada-Guillén, G. A., Riu, J., Düzgün, A., and Rius, F. X. (2009) Angew. Chem. Int. Ed. 48, 7334–7337.
[52] He, J., Liu, Y., Fan, M., and Liu, X. (2011) J. Agric. Food Chem. 59, 1582–1586.
[53] Revin, S. B., and John, S. A. (2011) Electrochim. Acta 56, 8934–8940.
[54] Liu, Y., Yuan, R., Chai, Y., Tang, D., Dai, J., and Zhong, X. (2006) Sens. Actuators B 115, 109–115.
[55] He, J.-B., Qi, F., Wang, Y., and Deng, N. (2010) Sens. Actuators B 145, 480–487.
[56] Charoenkitamorn, K., Chailapakul, O., and Siangproh, W. (2015) Talanta 132, 416–423.
[57] Istone, W. K. (1995) *X-Ray Photoelectron Spectroscopy* (XPS). Florida USA: CRC Press.
[58] Tığ, G. A., Zeybek, B., and Pekyardımcı, Ş. (2016) Talanta 154, 312–321.
[59] Kalimuthu, P., and John, S. A. (2009) Electrochem. Commun. 11, 367–370.
[60] Jin, D., Xu, Q., Yu, L., Mao, A., and Hu, X. (2016) Food Chem. 194, 959–965.
[61] Qi, Y., Xiu, F.-R., Zheng, M., and Li, B. (2016) Biosens. Bioelectron. 83, 243–249.
[62] Taghdisi, S. M., Danesh, N. M., Ramezani, M., and Abnous, K. (2017) Microchim. Acta 184, 499–505.
[63] Bahreyni, A., Yazdian-Robati, R., Ramezani, M., Abnous, K., and Taghdisi, S. M. (2018) Microchim. Acta 185, 272.
[64] Li, H., Hu, W., Hassan, M. M., Zhang, Z., and Chen, Q. (2019) J. Food Measur. Character. 13, 259–268.
[65] Fan, K., Kang, W., Qu, S., Li, L., Qu, B., and Lu, L. (2019) Talanta 197, 645–652.
[66] Lin, B., Yu, Y., Li, R., Cao, Y., and Guo, M. (2016) Sens. Actuators B 229, 100–109.
[67] Jiang, D., Du, X., Liu, Q., Zhou, L., Dai, L., and Qian, J., Wang, K. (2015) Analyst 140, 6404–6411.
[68] Bai, Y., Feng, F., Zhao, L., Wang, C., Wang, H., Tian, M., Qin, J., Duan, Y., and He, X. (2013) Biosens. Bioelectron. 47, 265–270.